NACA RM L50I20

NACA

RESEARCH MEMORANDUM

EXPERIMENTAL INVESTIGATION OF A FLAT-PLATE PADDLE JET VANE OPERATING ON A ROCKET JET

By Aleck C. Bond

Langley Aeronautical Laboratory
Langley Air Force Base, Va.

NATIONAL ADVISORY COMMITTEE
FOR AERONAUTICS

WASHINGTON

November 15, 1950
Declassified February 8, 1960

NACA RM L50I20

NATIONAL ADVISORY COMMITTEE FOR AERONAUTICS

RESEARCH MEMORANDUM

EXPERIMENTAL INVESTIGATION OF A FLAT-PLATE PADDLE JET VANE OPERATING ON A ROCKET JET

By Aleck C. Bond

SUMMARY

The results of static tests conducted for the purpose of determining the lift forces and hinge moments associated with a flat-plate paddle vane, externally hinged near a rocket-nozzle exit and operating on the jet, are presented for vane deflection angles ranging from -4° to 25°. The majority of the data presented is for a vane of aspect ratio 2; however, limited data are presented for vanes of aspect ratio 1 and $1\frac{1}{2}$. A 3.25-inch solid-fuel rocket motor was employed for the tests.

Lift forces of considerable magnitude were obtained with relatively high hinge moments. A maximum lift force of 198.5 pounds was obtained with a vane area of 4.134 square inches for a thrust of 2000 pounds and a vane deflection angle of 25°. The corresponding hinge moment was 155.7 inch-pounds. There was considerable rearward shift of the vane center of pressure with deflection angle. Lift and hinge-moment coefficients were found to increase with vane aspect ratio.

It was observed for vane deflections of 10° and greater that a change in rocket-pressure ratio from 40 to 45 and from 45 to 50 produces an approximate increase of 1° in the true angle of attack of the vane. This effect was attributed to the increase of the jet divergence angle with pressure ratio.

Evaluation of the rocket performance with and without vane indicated that the performance of the rocket motor was not appreciably affected by the presence of the vane in the stream. The mean loss of specific impulse for all firings was only 1.37 percent.

Vanes were reused for an average of six firings without any noticeable erosion of the vane surface. The absence of noticeable vane erosion was attributed mainly to the short action time of the rocket motor of only 1.1 seconds. The material used for the vanes was 18-8 stainless steel.

INTRODUCTION

The deflection of a jet can be utilized to provide stability and control for a jet-propelled aircraft. The feasibility of utilizing forces available in a deflected jet for stability and control may be demonstrated by the results of tests reported in references 1 and 2. It is believed that considerable gain in performance could be made by the use of jet controls in lieu of the conventional fixed fin controls. This would be especially true in the case of a booster-model combination where very large booster-fin areas are required for stabilization. Jet deflection is especially adapted for control during launching when airspeeds are so low that external controls are effective only with excessively large fin areas. Reduction of fin area to that necessary for normal flight could be effected if internal controls were employed during launching. Another application for control by jet deflection is that of flight at extreme altitudes where the rarefied atmosphere makes external control ineffective.

There are numerous ways of diverting a high-velocity jet from a given direction, including swiveling nozzles, immersed vanes, paddle vanes, and many others (as reported in reference 3). However, up to the present time, experimental studies of the various methods have been limited. Some experimental work on immersed vanes for specific applications has been done. (See references 4 and 5.) The purpose of the present investigation was the determination of the forces and moments associated with a flat-plate paddle vane externally hinged near a rocket-nozzle exit and operating on the jet. The experimental investigation conducted by the Langley Pilotless Aircraft Research Division utilized a two-component thrust stand.

SYMBOLS

T	thrust, pounds
P	pressure, pounds per square inch
t	time, seconds
I	impulse, pound-seconds $\left(\int_0^t T\,dt\right)$
I_{sp}	specific impulse, pound-seconds per pound $\left(I_T/W\right)$

w_p	expended weight of propellant at any time, t, pounds
w_i	igniter weight, pounds
W	total weight of propellant, pounds
M	mass rate of flow, slugs per second (ρAV)
ρ	density, slugs per cubic foot
A	cross-sectional area, square feet
V	linear velocity, feet per second
C_L	lift coefficient (L/qS)
C_D	drag coefficient (D/qS)
F	net vertical force measured by thrust stand, pounds
R	resultant pressure force on vane, pounds
L	lift, pounds
D	drag, pounds
d	perpendicular distance from vane surface to hinge point, inches
q	dynamic pressure, pounds per square foot $\left(\frac{1}{2}\rho V^2\right)$
A	aspect ratio (b/c)
S	vane surface area, square feet (bc/144)
b	vane span (equal to rocket-nozzle-exit diameter), inches
C_h	hinge-moment coefficient (H/qSc)
H	hinge moment, inch-pounds
c	vane chord, inches (see fig. 1)
δ	vane deflection angle or angle made by vane surface and nozzle divergence half angle, degrees

α angle made by vane surface and longitudinal axis of rocket motor, degrees

c.p. center of pressure, percent chord

l vane immersion length for variable immersion vane, inches (equal to c)

Subscripts:

e exit of nozzle

T total

c chamber

a ambient

p pressure

f friction

TEST APPARATUS AND INSTRUMENTATION

Jet-Vane Test Assembly

The jet-vane test assembly consists primarily of a vane adapter, a strain-gage beam and support, and an arm for transferring the vane hinge moments to the strain-gage beam. The jet-vane test assembly (with one beam support plate removed) mounted on a 3.25-inch standard aircraft rocket motor is shown in figure 2. The vane adapter is hinged near the rocket-nozzle exit and the vane is attached to the adapter. Provision for changing the deflection angle of the vane between firings was incorporated in the beam support plates by changing the location of the strain-gage beam (an adjustable contact point at the end of the arm being used for fine adjustment of δ). Zero deflection angle was arbitrarily chosen so as to coincide with the nozzle divergence half angle of the rocket motor. A schematic sketch of the jet vane relative to the rocket nozzle, giving zero, maximum, and minimum deflection angles, is shown in figure 3.

The vane was designed as an insert instead of as an integral part of the assembly in order to simplify replacement of eroded vanes. A sketch giving the jet-vane dimensions for the three aspect ratios tested is shown in figure 1. The leading edge of the vane was rounded in order to direct any of the expanding flow from the nozzle along the surface of

the vane and to prevent leakage of the gases about the leading edge. The leading edge, however, was considered ineffective and the effective chord of the vane was assumed to be the flat portion to the rear of the point of tangency. The three values of aspect ratio 1, $1\frac{1}{2}$, and 2 were obtained by maintaining the span of the vane constant (equal to the rocket-nozzle-exit diameter) and changing the effective chord of the vane accordingly. The vane was machined from a solid block of 18-8 stainless steel. This material was used because of its relatively good high-temperature heat-resisting qualities.

The strain-gage beam employed in this application was used to measure hinge moments about the hinge line of the vane. This beam was calibrated by applying load through a contact point on the center line of the vane at a given distance from the hinge line. The load was applied by means of a jack arrangement through a ring dynamometer (as shown in fig. 4). Calibrations were made at each vane deflection angle in order to eliminate any errors due to machining.

Thrust Stand

The thrust stand used for this series of tests was designed to measure two components of force - thrust and lift. Thrust is measured along a line lying in the horizontal plane, and lift is measured on a vertical line perpendicular to the thrust line. Lift and thrust loads were measured by means of strain-gage-beam components designed to transmit the applied loads. The strain-gage beams were designed so that the range of applied loads would develop adequate elastic strains in the beams to produce the necessary electrical output from the gages for maximum accuracy. A photograph of the thrust stand as set up for the jet-vane tests and giving the locations of the lift and thrust beams is shown in figure 5(a).

The thrust line of the rocket motor is assumed to coincide with the geometrical center line of the motor. Calibration of the thrust component was accomplished by means of a calibrating rig designed to aline applied loads with the geometric center line of the rocket motor. The setup for calibration of the thrust component is shown in figure 5(b). Lift interaction on the thrust component was found to be too small to measure. The lift component was calibrated by applying loads in the vertical direction, perpendicular to the geometrical center line of a rocket case supported in the stand. A photograph of the calibration of the lift component is shown in figure 5(c). The results of several lift calibrations made by loading the rocket case at several stations along its center line indicated that the calibration factor remained constant regardless of the point of application of the load. Thrust interaction on the lift component was found to be negligible (less than 1/2 percent in the high-lift range.)

Rocket Motor

The 3.25-inch aircraft rocket motor, Mk 7, with a modified Mk 13 propellant grain, was used throughout this series of tests. The Mk 13 grain is of cruciform configuration with 46.6 percent of the outer arm area inhibited to provide neutral burning. (See reference 6.) The grain was modified to provide a progressive burning rocket (thrust increasing with time) and hence a wide range of thrust values. This was desirable in correlating the vane aerodynamic data over a range of thrust values. Modification of the grain consisted of increasing the inhibiting of the outer arm area to 70.2 percent.

The following rocket-motor data are presented as being pertinent to the jet-vane investigation. Further information may be found in references 7 and 8.

Powder type	JPN
Average powder weight, pounds	8.50
Nozzle-throat diameter, inches	1.50
Nozzle-exit diameter, inches	2.875
Average action time at 75° F, seconds	1.10
Approximate range of thrust, pounds	1400 to 2100
Approximate range of chamber pressure, psia	515 to 772
Mach number at nozzle exit (approximate)	2.62
Isobaric adiabatic flame temperature of powder, °F (reference 9)	4990
Ratio of specific heats of exhaust gases, γ (computed by method of reference 9)	1.219

Instrumentation

The majority of the pressure measurements was made using electrical pressure transmitters which utilize electrical strain gages for converting pressure impulses to electrical impulses; however, a few of the measurements were made using an optical-type pressure recorder which incorporates a pressure transmitter and recording system. Calibration of the pressure transmitters was accomplished by means of a dead-weight tester.

The electrical output from the thrust, lift, and hinge-moment strain gages and the electrical pressure transmitter was recorded by means of a recording galvanometer on a 6-inch-wide strip of photographic paper. The optical-type pressure recorder provided the pressure data on a $2\frac{7}{16}$-inch-wide strip of photographic film. An electric timer incorporated in the system impressed timing marks on the records at $\frac{1}{10}$-second intervals,

thus correlating all data with respect to time. Reduction of the data involved the reading of the gross deflections from a given reference line, computing the net deflections, and applying the appropriate calibration factor.

A number of the firings were photographed using either a 16-millimeter or 35-millimeter high-speed motion-picture camera in order to provide qualitative information on the flow pattern of the jet over the vanes.

Tests

A total of 23 rocket firings was made for this series of tests. A record of all firings is presented in table I. The vane deflection angle was held constant for each of the tests. Firings 1 to 18 were made with a vane of aspect ratio 2 and covered a range of vane deflection angles from -4° to 25°. Firings 19 and 20 were made with vanes of aspect ratios $1\frac{1}{2}$ and 1, respectively, at a vane deflection angle of 15°. The remaining three firings were made for the purpose of determining the performance of the rocket motor without the jet vane.

In each of the jet-vane tests, with the exception of firing 17, the thrust varied over an approximate range from 1,400 to 2,100 pounds. The range of exit pressures resulting from this range of thrust was 22.4 to 33.6 pounds per square inch absolute. Firing 17 covered a thrust range of approximately 1,000 to 1,500 pounds. This was accomplished by cutting the length of the propellant grain from 33.80 inches to 28.50 inches and by maintaining the 70.2 percent inhibiting of the outer arm area. This range of thrust provided exit pressures from 16 to 24 pounds per square inch absolute. The purpose of firing 17 was therefore to investigate any variation in vane lift due to expansion to near atmospheric pressures at the nozzle exit.

Measurements of lift, vane hinge moment, and rocket thrust were made during each of the jet-vane tests. Measurements of the chamber pressure at the nozzle entrance were made during each test, with the exception of firing 4. Also, during two firings, measurements of pressure at the nozzle exit were made in order to check the computed value of the ratio of the chamber pressure to exit pressure. Certain other data, as indicated by table I, were excluded since the accuracy was impaired by instrumentation difficulties experienced in these tests. A time history of firing 12 is presented in figure 6 as being typical of data obtained from the tests.

Corrections

As previously mentioned, the lift force measured by the thrust stand lies in a vertical plane and hence it is necessary to correct the net vertical force by the weight of the expended propellant plus igniter. The igniter weight is assumed to be expended instantaneously at the instant of ignition and hence the correction is constant throughout. The correction for the expended propellant weight is not constant, however, and varies from zero prior to the instant of ignition to a maximum W, the total weight of the propellant, at the end of firing. It was therefore assumed that the expended weight of propellant w_p at any time between ignition and end of firing was directly proportional to the impulse realized up to that time, the inverse of the specific impulse being the factor of proportionality. Expressed in the form of an equation, the expended weight of propellant at any time t is

$$w_p = \frac{W}{I_T} I$$

where I is the impulse realized at time t and $\frac{W}{I_T}$ is the inverse of the specific impulse of the firing. The vane lift force therefore may be expressed as

$$L = F - \left(w_p + w_i\right)$$

where F is the net vertical force measured by the thrust stand.

RESULTS AND DISCUSSION

Vane Aerodynamic Characteristics

The lift and hinge-moment data are presented in the form of dimenionless coefficients, which are based on the instantaneous dynamic pressure at the nozzle exit q_e determined as shown in appendix A.

Curves of vane lift coefficient as a function of thrust for constant vane deflection angles for the aspect-ratio-2 vane are presented in figure 7. The lift coefficients are based on a vane surface area of 4.134 square inches. These curves indicate an almost linear variation of lift coefficient with thrust, the curves of the higher deflection angles being more nearly linear. This increase in lift coefficient

with thrust for constant deflection angle is attributed to the increase in jet divergence angle with thrust, which in effect increases the true angle of attack of the vane. The experimental data of figure 7 are cross-plotted in figure 8 and are presented as faired curves of lift coefficient as a function of vane deflection angle (deviation from the nozzle divergence half angle as shown in fig. 3) for constant values of thrust equal to 1,600, 1,800, and 2,000 pounds, which correspond to ratios of P_c/P_a of 40, 45, and 50, respectively. These curves indicate a relatively low rate of change of lift coefficient with vane deflection angle for the negative and smaller positive vane deflection angles which increases with positive vane deflection angles and becomes nearly constant above 10°. It is seen, therefore, that the vane is less effective for the negative and smaller positive deflection angles and becomes almost fully effective for angles of 10° and greater. This lack of effectiveness of the vane at negative and smaller positive deflection angles may be explained by the fact that only a small portion of the vane surface is immersed in the stream at these small angles. The curves of figure 8 also show clearly the effective increase in angle of attack corresponding to an increase in thrust. For vane deflection angles of 10° or greater, the incremental change in lift coefficient obtained by increasing or decreasing the thrust by 200 pounds from 1,800 pounds is the same as the increment of lift coefficient realized by increasing or decreasing the vane deflection angle by approximately 1°. This therefore indicates that changing the thrust from 1,600 to 1,800 pounds or from 1,800 to 2,000 pounds produces approximately 1° change in jet divergence angle, which in effect constitutes a 1° change in true angle of attack of the vane. Calculation of the jet divergence angle by means of two-dimensional-flow theory for values of P_c/P_a of 40, 45, and 50 indicated an increase of approximately 0.9° in jet divergence angle for an increase in P_c/P_a from 40 to 45 and from 45 to 50. The change in jet divergence angle, measured from motion pictures made during several of the firings, was also approximately 1° for these changes in pressure ratio.

The lift data of the low-pressure firing (firing 17) are also presented in figure 7. These data show no irregularities in vane lift due to expansion to near atmospheric pressures at the nozzle exit for 20° deflection.

Curves of hinge-moment coefficient as a function of thrust for constant vane deflection angles, for the aspect-ratio-2 vane, are presented in figure 9. The hinge-moment coefficients are based on a vane chord of 1.438 inches. Similarly, as in the case of the lift-coefficient curves, these curves indicate almost linear variation of hinge-moment coefficient with thrust. The experimental data of figure 9 are cross-plotted in figure 10 and are presented as faired curves of hinge-moment

coefficient as a function of vane deflection angle for constant values of thrust. These curves show an increase in hinge moment with vane deflection angle as was expected.

A maximum lift force of 198.5 pounds was obtained for a thrust of 2,000 pounds and a vane deflection angle of 25°. The corresponding hinge moment was 155.7 inch-pounds. A curve of the variation of lift coefficient with hinge-moment coefficient for constant values of thrust is presented in figure 11. Values of dynamic pressure for the purpose of calculation are 117.8, 132.1, and 145.4 pounds per square inch for thrusts of 1,600, 1,800, and 2,000 pounds, respectively.

The center of pressure of the vane (fig. 12) was determined by means of equation (5) given in appendix B. A plot of center of pressure as a function of vane deflection angle for the various thrust values is presented in figure 13. These curves indicate considerable shift in center of pressure with vane deflection angle for the range of angles covered, the rate of shift being high for the smaller deflection angles and becoming less for the larger deflection angles. The shift in center of pressure may be attributed to the velocity distribution of the jet and the increase in trailing-edge effective area with deflection angle. At small deflection angles the vane is operating in the lower velocity region of the jet and only a small portion of the vane surface is actually effective. As the deflection is increased, the trailing edge becomes increasingly effective, in addition to the fact that it is operating in a higher velocity region and hence shifts the center of pressure rearward. As the deflection is further increased, the forward portion of the vane begins to gain effectiveness and the rate of rearward shift of center of pressure decreases, now being influenced mainly by the velocity distribution of the jet.

Photographs showing the action of the jet on the vane of aspect ratio 2 for deflection angles of 10° and 20° are presented in figure 14. The shock wave from the leading edge of the vane and the jet spreading characteristics were clearly defined in the original film; however, these photographs were used to provide only qualitative information on the operation of the vane in the jet.

As previously mentioned, firings 19 and 20 were made with vanes of aspect ratios $1\frac{1}{2}$ and 1, respectively, at a vane deflection angle of 15°. The purpose of these two tests was to determine the effect of aspect ratio on the aerodynamic characteristics of the paddle jet vane. Curves of vane lift coefficient as a function of thrust for the three aspect ratios tested at a δ of 15° are presented in figure 15. These lift coefficients are based on vane surface areas of 5.511 and 8.266 square inches for aspect ratios of $1\frac{1}{2}$ and 1, respectively. Also, the curves

of vane hinge-moment coefficient as a function of thrust for the three aspect ratios tested at a δ of 15° are presented in figure 16. These hinge-moment coefficients are based on vane chords of 1.917 and 2.875 inches for aspect ratios of $1\frac{1}{2}$ and 1, respectively. The curves of C_L and C_h as a function of thrust for the vane of aspect ratio 2 at a δ of 15° were repeated in figures 15 and 16, respectively, for purposes of comparison. The observations made with respect to the lift and hinge-moment data for the vane of aspect ratio 2 are also applicable to these data and hence will not be restated. The effect of aspect ratio on vane lift coefficient for a vane deflection angle of 15° and values of thrust of 1,600, 1,800, and 2,000 pounds is shown in figure 17; likewise, the effect of aspect ratio on the corresponding hinge-moment coefficient is presented in figure 18. The effect, therefore, is an increase in both the lift and hinge-moment coefficients with aspect ratio.

In addition to providing data on the flat-plate paddle jet vane, the data of figure 17 may be interpreted so that they may be applied to another type of control vane, the variable immersion vane. This type of control vane would not be hinged but would slide in and out of the jet blast at some constant deflection angle and the control force provided would depend on the immersed vane area and thrust. This type of control vane would reduce the high operating forces of the paddle vanes. A sketch of the variable immersion scheme is shown in figure 19. The data of figure 17 are presented in another form, lift coefficient times vane area as function of length of vane immersion, in figure 20 in order to show the effect of immersed vane length on the available lift. These curves show an increase in lift force with immersed vane length, as would be expected.

It must be kept in mind that the foregoing data are applicable to the case where the vane span is equal to the nozzle-exit diameter and that, for a vane of different span, the data are not directly applicable, since the vane edge conditions would not necessarily be the same.

Performance of Rocket Motor

The performance of a solid-propellant rocket motor is generally expressed in terms of specific impulse, which is the impulse delivered per unit weight of propellant consumed. The loss incurred in specific impulse for each of the vane firings is presented in table I and is based on a reference value of specific impulse, which is the average of values obtained from three firings without vane. Also included in table I is the percentage loss in specific impulse based on the reference value. The mean loss of specific impulse for all firings was only 1.37 percent. Firings at lesser deflection angles indicated smaller losses; however, the trend of the results is not uniform. This may be observed more clearly

in figure 21, which is a plot of specific impulse realized from firings with jet vane at the various deflection angles compared with the reference value of specific impulse without vane. The low impulse values obtained for the deflection angles of -4°, 4°, and 6° may be due to the ejection of unburned grain slivers through the nozzle. The scatter observed in the specific impulse values for the higher deflection angles may be due to a number of possibilities; namely, (1) errors in weighing the propellant grains, (2) errors in reading of records and determining values of impulse, and (3) slight variations in nozzle geometry, and others.

Vane Erosion

Erosion of the vanes, which is generally encountered in jet-vane applications, presented no problem for this particular application. The material used for the vanes was 18-8 stainless steel. Vanes were reused for an average of six firings without any noticeable erosion. It is true, of course, that, since the average action time was only 1.1 seconds, no excessive erosion should be expected. An additional factor contributing to the absence of noticeable erosion was the fact that the vane was operating at the outer fringes of the jet boundary and was therefore out of the high-temperature region of the jet.

CONCLUSIONS

From the foregoing discussion of the results of the tests with the flat-plate paddle jet vane the following conclusions may be drawn:

1. Lift forces of a considerable magnitude may be obtained with a flat-plate paddle jet-vane configuration externally hinged near a rocket-nozzle exit and operating on the jet. In addition, the hinge moments of such a configuration are high, in comparison with a vane hinged near the center of pressure.

2. For vane deflection angles of 10° and higher, an increase in rocket-pressure ratio from 40 to 45 and from 45 to 50, produced an approximate increase of 1° in the true angle of attack of the vane. This effect was attributed to the increase of the jet divergence angle with pressure ratio.

3. There was considerable rearward shift of center of pressure with deflection angle. The center of pressure varied from approximately 18 to 53 percent chord, for an aspect-ratio-2 vane, as the vane deflection angle was increased from 4° to 25°.

4. Lift and hinge-moment coefficients were found to increase with vane aspect ratio (for a vane span equal to the nozzle-exit diameter) at a vane deflection angle of 15°.

5. The performance of the rocket motor was not appreciably affected by the presence of the vane in the stream.

6. There was no indication of irregularities in vane lift due to expansion to near atmospheric pressures at the nozzle exit for a 20° vane deflection.

7. No erosion of the paddle vane was experienced with the short burning rocket used in the present tests.

Langley Aeronautical Laboratory
National Advisory Committee for Aeronautics
Langley Air Force Base, Va.

APPENDIX A

DETERMINATION OF DYNAMIC PRESSURE AT THE NOZZLE EXIT

The dynamic pressure at the nozzle exit q_e upon which the dimensionless coefficients C_L and C_h are based was computed in the following manner: Assuming that the pressure and velocity at the nozzle exit are constant across the jet, the thrust of a rocket motor for practical considerations may be expressed by the equation

$$T = 144(P_e - P_a)A_e + MV_e$$

from which the dynamic pressure at the nozzle exit may be derived as follows: Substituting $\rho_e A_e V_e$ for M and dividing through by 2 yields

$$\frac{1}{2}T = \frac{144}{2}(P_e - P_a)A_e + \frac{1}{2}\rho_e A_e V_e^2$$

Dividing through by A_e and transposing results in

$$\frac{1}{2}\rho_e V_e^2 = \frac{1}{2}\left[\frac{T}{A_e} - 144(P_e - P_a)\right]$$

and therefore

$$q_e = \frac{1}{2}\left[\frac{T}{A_e} - 144(P_e - P_a)\right]$$

Hence, it is seen that the dynamic pressure at the nozzle exit may be found knowing the values of T, P_e, and P_a. The value of P_e was calculated from P_c and the experimentally determined ratio of P_c/P_e. The average experimental value of $\frac{P_c}{P_e} = 23$ obtained from two firings was used and was found to agree favorably with the computed value. A value of 14.7 psi was used for P_a.

APPENDIX B

DETERMINATION OF VANE CENTER OF PRESSURE

Since the drag of the vane was not measured in the test, it was necessary to calculate drag in order to determine the center of pressure of the vane. The total drag of the vane is composed of pressure drag plus friction drag. Since the configuration is a flat plate, the resultant pressure force on the vane is perpendicular to the surface of the vane, and the friction drag force is parallel to the surface of the vane (as shown in fig. 12). The hinge moment of the vane is obtained by taking moments about the hinge point.

$$HM = R(c.p. \times c) + D_f \times d \tag{1}$$

From the figure

$$R = \frac{L_T}{\cos \alpha} \tag{2}$$

Therefore

$$HM = \frac{L_T}{\cos \alpha} (c.p. \times c) + D_f \times d$$

Transposing and multiplying by $\frac{\cos \alpha}{L_T}$

$$c.p. \times c = \frac{\cos \alpha}{L_T}\left(HM - D_f \times d\right) \tag{3}$$

The lift force measured by the thrust stand is the total lift of the vane less the vertical component of the friction drag. Therefore

$$L = L_T - D_f \sin \alpha$$

and

$$L_T = L + D_f \sin \alpha \tag{4}$$

Substituting for L_T in equation (3)

$$c.p. \times c = \frac{\cos \alpha \left(HM - D_f \times d\right)}{L + D_f \sin \alpha}$$

Multiplying by $\frac{qS}{qS}$

$$c.p. \times c = \frac{\cos \alpha \left(\frac{HM}{qS} \times \frac{c}{c} - \frac{D_f \times d}{qS}\right)}{\left(\frac{L}{qS} + \frac{D_f}{qS} \sin \alpha\right)}$$

Therefore

$$c.p. = \frac{\cos \alpha}{c} \times \frac{\left(c \times C_h - d \times C_{D_f}\right)}{\left(C_L + C_{D_f} \sin \alpha\right)} \qquad (5)$$

For this analysis, friction-drag coefficients were obtained by the method of reference 10. Calculated values of Reynolds number used in the determination of the friction-drag coefficients were 5.8×10^5, 6.5×10^5, and 7.4×10^5 for thrust values of 1,600, 1,800, and 2,000 pounds, respectively.

REFERENCES

1. Friedman, Henry: Summary Report on A-4 Control and Stability. Summary Rep. No. F-SU-2152-ND, Air Materiel Command, U. S. Army Air Forces, June 1947.

2. Rosan, H. J.: LTV-N-4b1 (VTV-1) Design, Development, and Flight Test. CAL/CM-547, CAL-1-D-2, Cornell Aero. Lab., May 27, 1949.

3. Rose, C. H., and Immenshuh, W. I.: Report on Engineering Study and Investigation of the Problems of Jet-Thrust Systems As Related to Control of an Airplane. Pts. I and II. Rep. No. 3817-6, Ryan Aero. Co., April 28, 1948.

4. Main, J. H., and Winer, R.: Studies of Jet-Vanes in Rockets. Allegany Ballistics Lab. Rep. ABL A-4 No. 2, Bur. Ordnance, Oct. 1948.

5. Powell, W. B.: Experimental Investigations with Jet Control Vanes. Progress Rep. No. 4-30, Jet Propulsion Lab., C.I.T., 1948.

6. Sage, B. H.: Development of the Mk 13 Cruciform Propellant Grain. OSRD, C.I.T., NDRC, Div. 3, Sec. L, Dec. 29, 1943.

7. Anon.: Internal and External Ballistic Data - Fin-Stabilized Rockets. OSRD Rep. No. 2409, C.I.T., UBC 28, NDRC, Div. 3, Sec. L, March 15, 1945.

8. Anon.: Jato Manual. SPIA/M1, The Johns Hopkins Univ., Appl. Phy. Lab., March 1949.

9. Anon.: Rocket Fundamentals. OSRD No. 3992, ABL-SR4, NDRC, Div. 3, Sec. H, 1944.

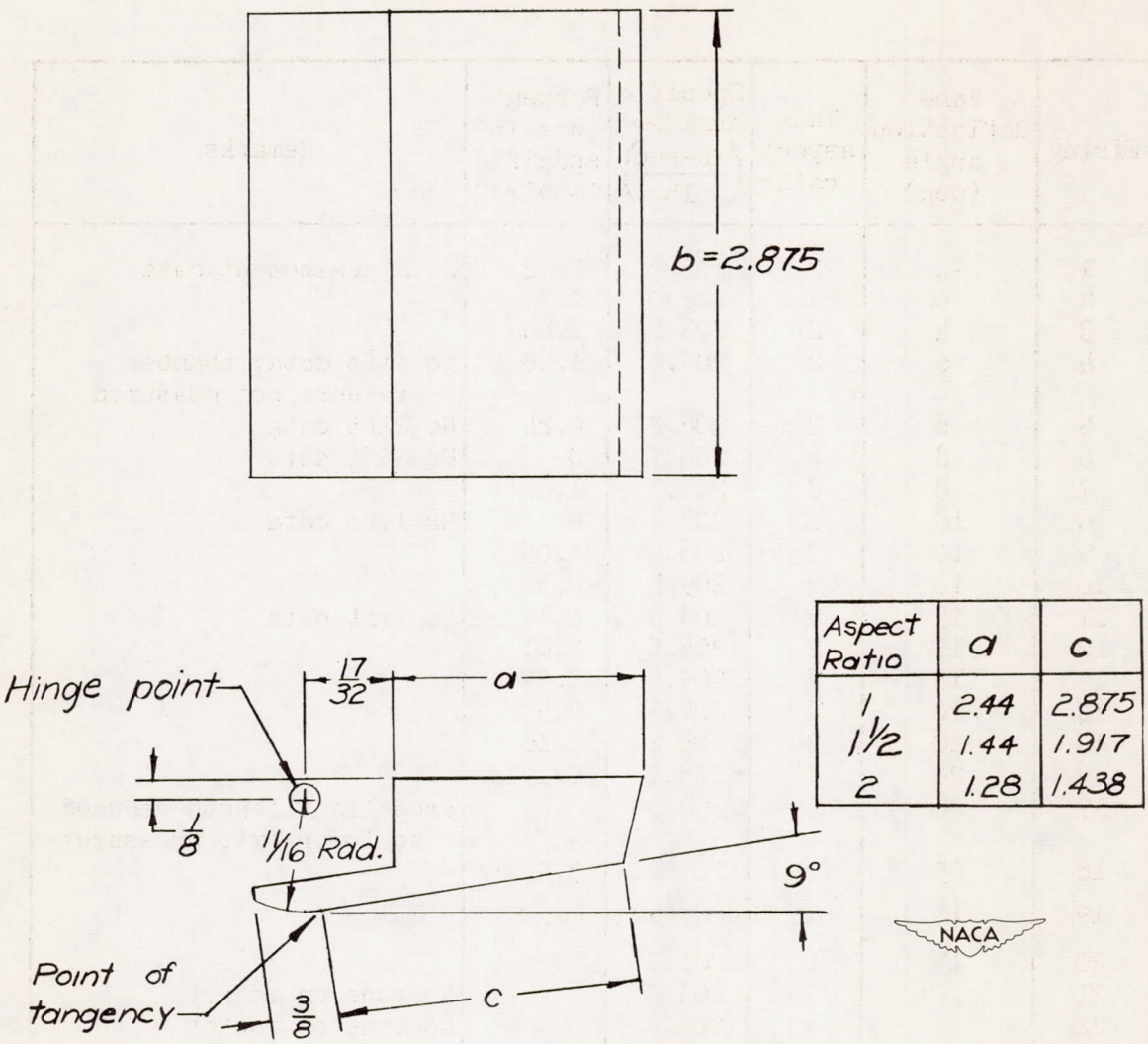
10. Falkner, V. M.: A New Law for Calculating Drag. The Resistance of a Smooth Flat Plate with Turbulent Boundary Layer. Aircraft Engineering, vol. XV, no. 169, March 1943, pp. 65-69.

TABLE I

RECORD OF FIRINGS INCLUDING LOSS IN SPECIFIC IMPULSE FOR VARIOUS VANE DEFLECTION ANGLES

Firing	Vane deflection angle (deg)	Vane aspect ratio	Specific impulse $\left(\frac{\text{lb-sec}}{\text{lb}}\right)$	Percent loss in specific impulse[a]	Remarks
1	-4	2	203.2	2.64	No hinge-moment data
2	0	2	208.0	0.34	
3	4	2	203.6	2.44	
4	6	2	205.6	1.48	No lift data; chamber pressure not measured
5	8	2	208.2	0.24	No lift data
6	8	2	208.7	0	No lift data
7	8	2	205.7	1.44	
8	10	2	208.7	0	No lift data
9	10	2	206.5	1.05	
10	10	2	209.5	-0.38	
11	15	2	208.3	0.19	No lift data
12	15	2	204.5	2.01	
13	15	2	205.8	1.39	
14	20	2	207.6	0.53	
15	20	2	204.2	2.16	
16	20	2	208.3	0.19	
17	20	2	204.0	2.25	Propellant length reduced to lower exit pressures
18	25	2	201.2	3.59	
19	15	$1\frac{1}{2}$	203.9	2.30	
20	15	1	201.5	3.50	
21			208.2		No vane on rocket
22			208.2		No vane on rocket
23			209.8		No vane on rocket

[a]This loss in specific impulse is based on a reference value of 208.7 lb-sec/lb which is the average of values obtained from three firings without vane (firings 21, 22, and 23).



Aspect Ratio	a	c
1	2.44	2.875
1½	1.44	1.917
2	1.28	1.438

Figure 1.- Jet-vane dimensions. All dimensions are in inches.

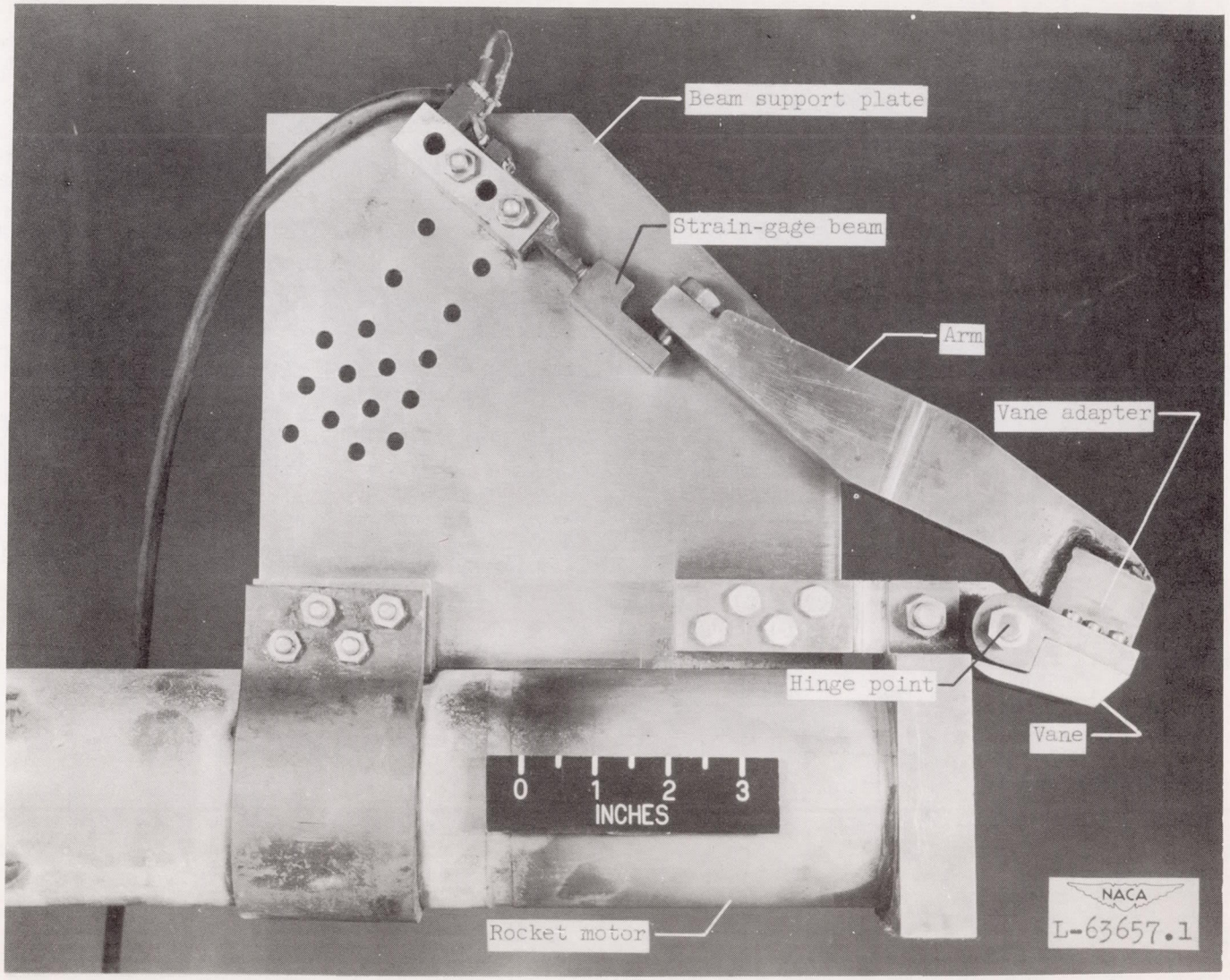


Figure 2.- Jet-vane test assembly (one beam support plate removed) mounted on 3.25-inch aircraft rocket motor.

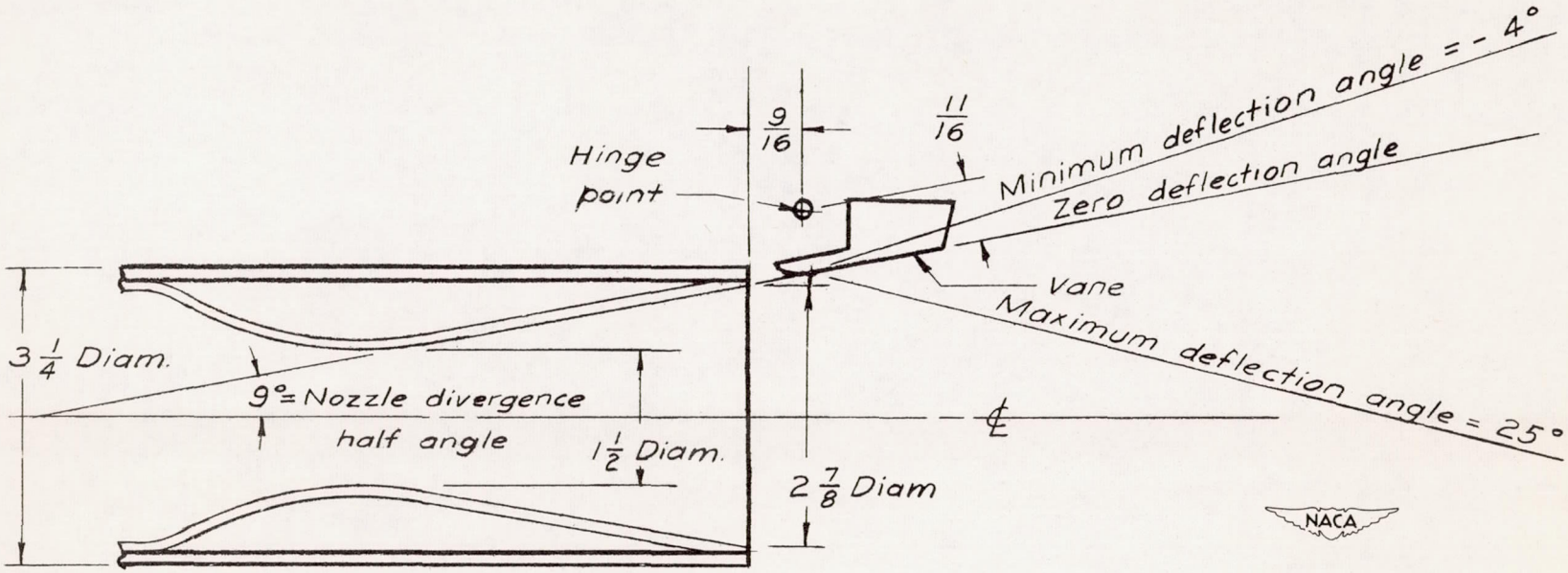


Figure 3.- Schematic sketch of jet vane relative to rocket nozzle showing zero, maximum, and minimum deflection angles. All dimensions are in inches.

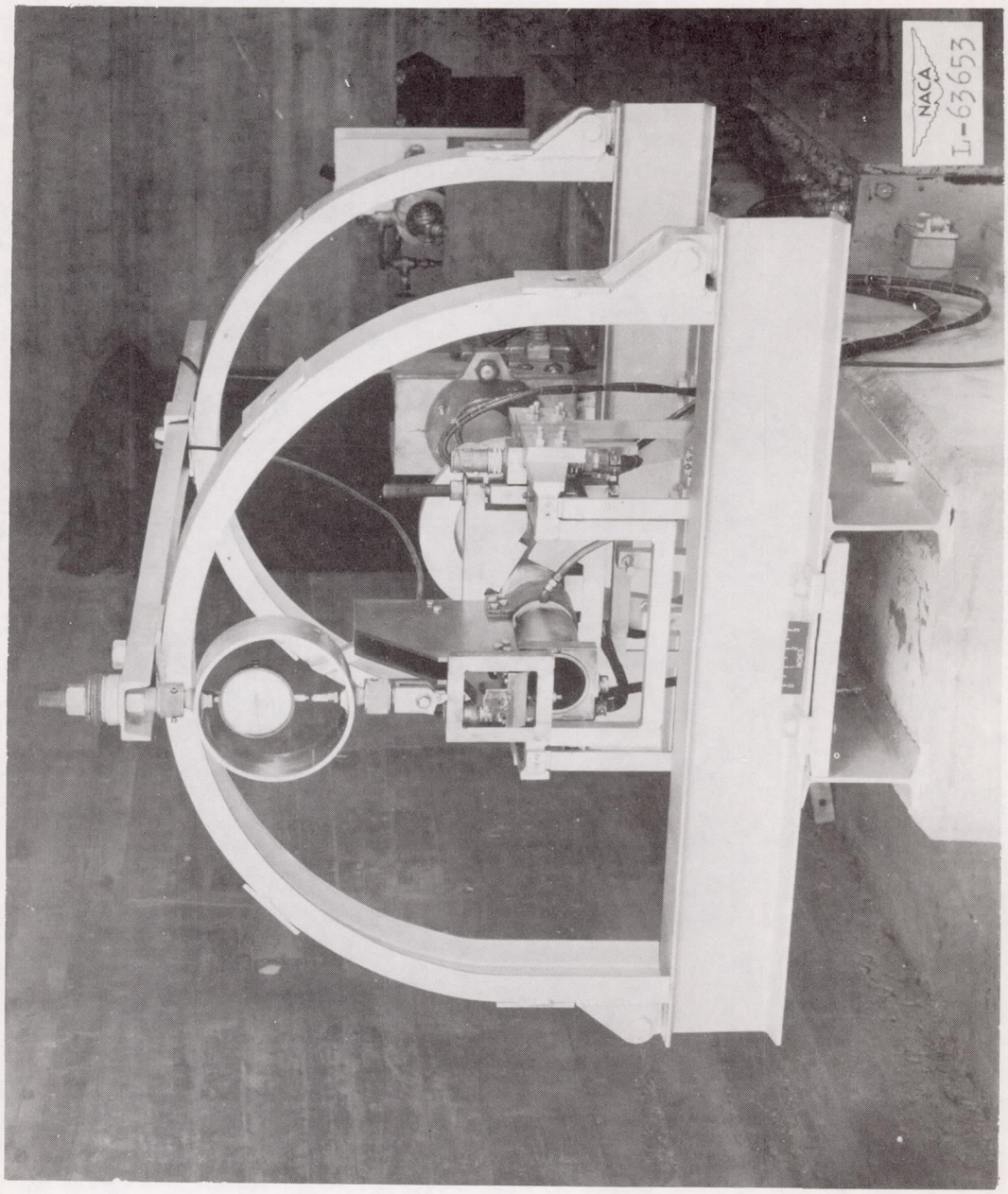
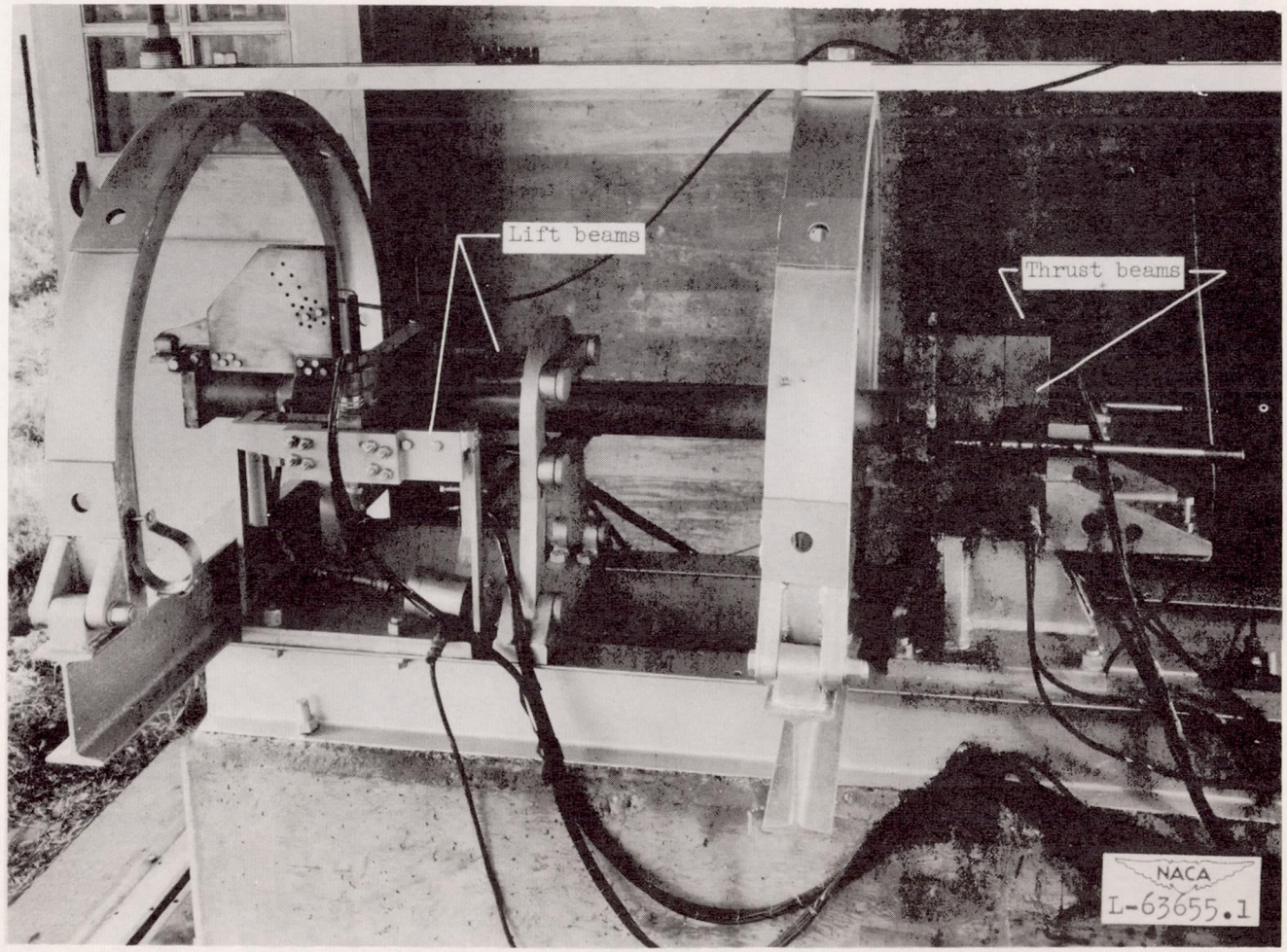
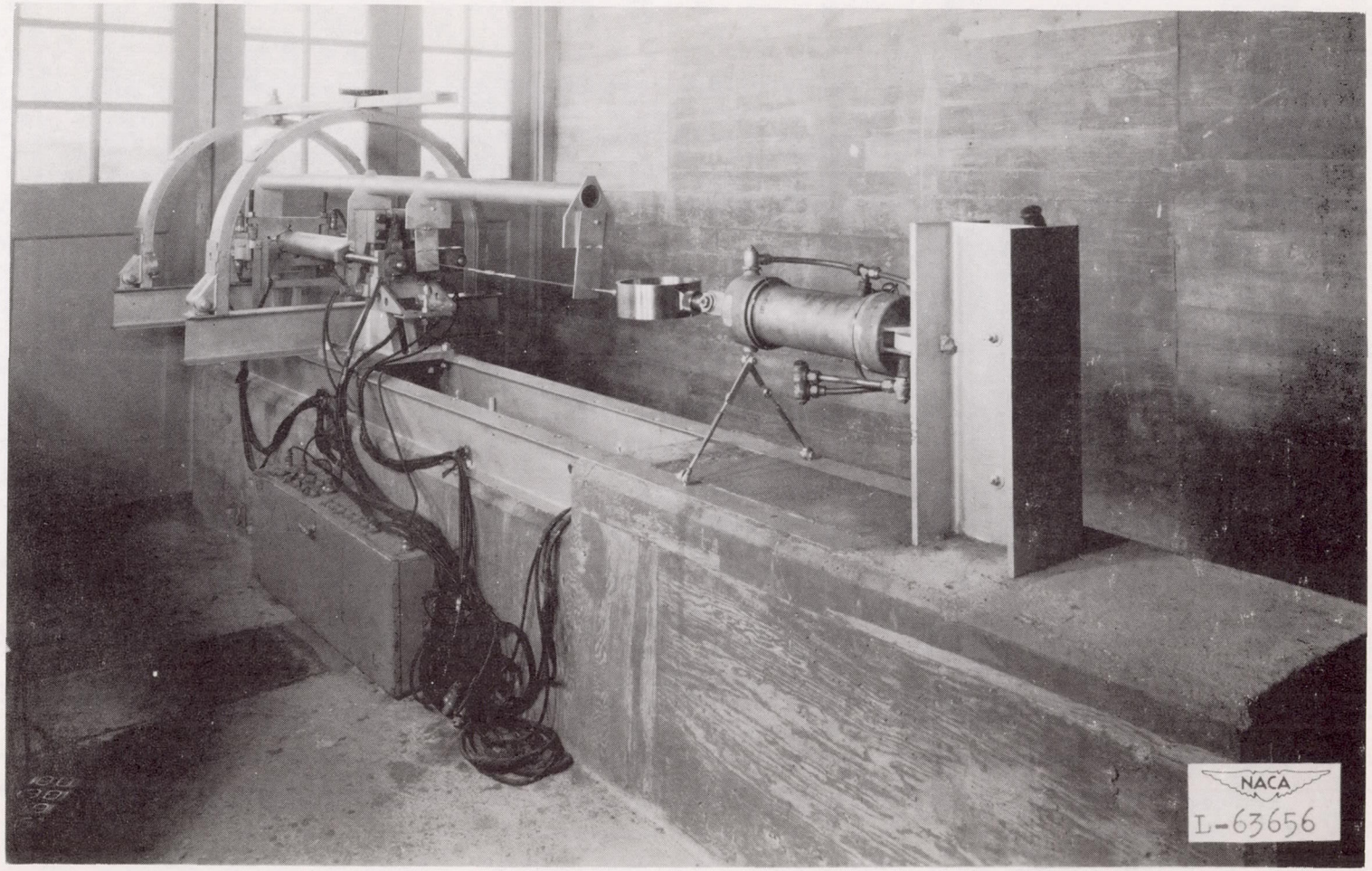


Figure 4.- Calibration of hinge-moment beam.



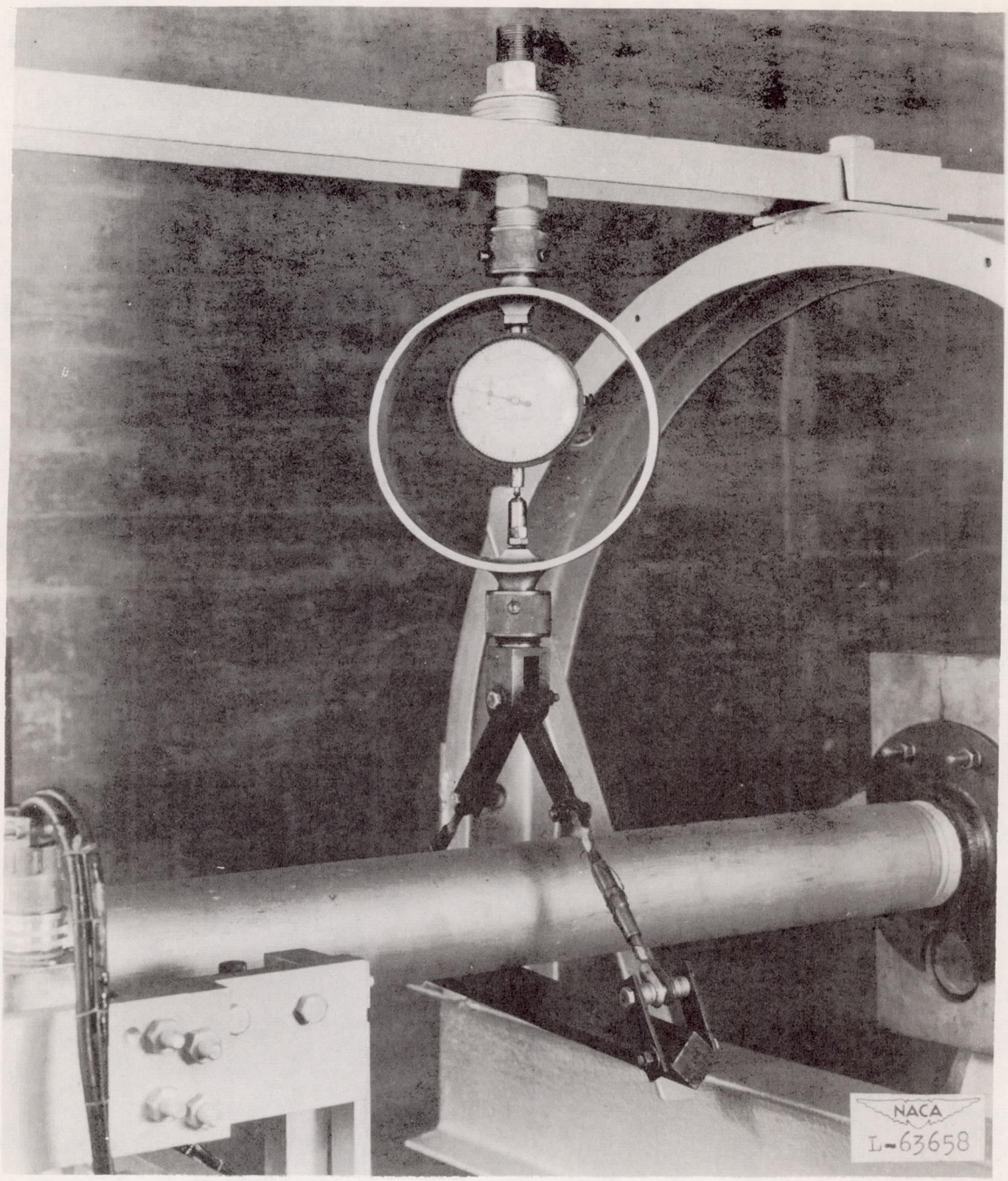
(a) Thrust stand as set up for jet-vane tests. Location of lift and thrust strain-gage beams shown.

Figure 5.- Thrust stand.



(b) Setup for calibration of thrust component.

Figure 5.- Continued.



(c) Setup for calibration of lift component.

Figure 5.- Concluded.

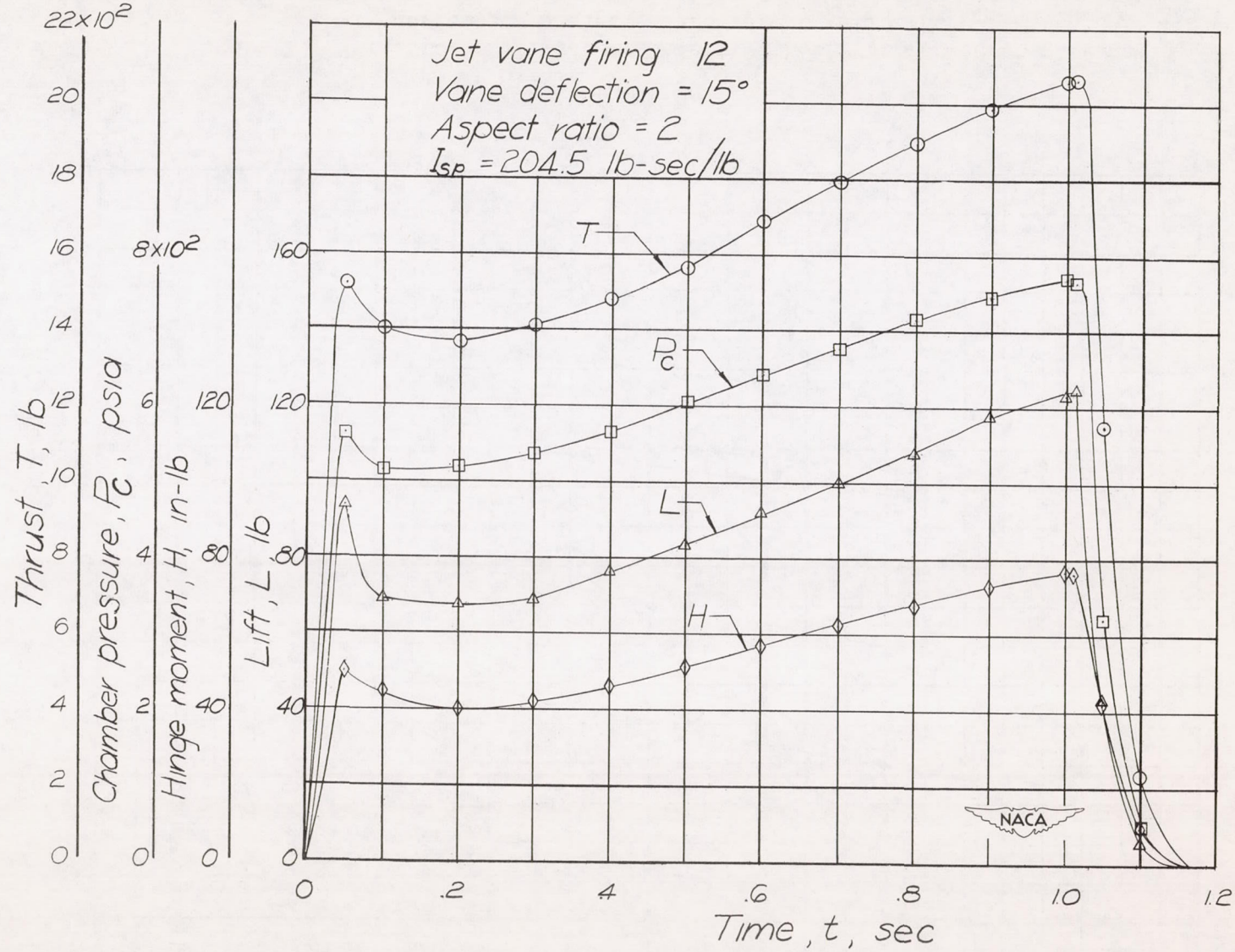


Figure 6.- Typical set of data obtained from tests.

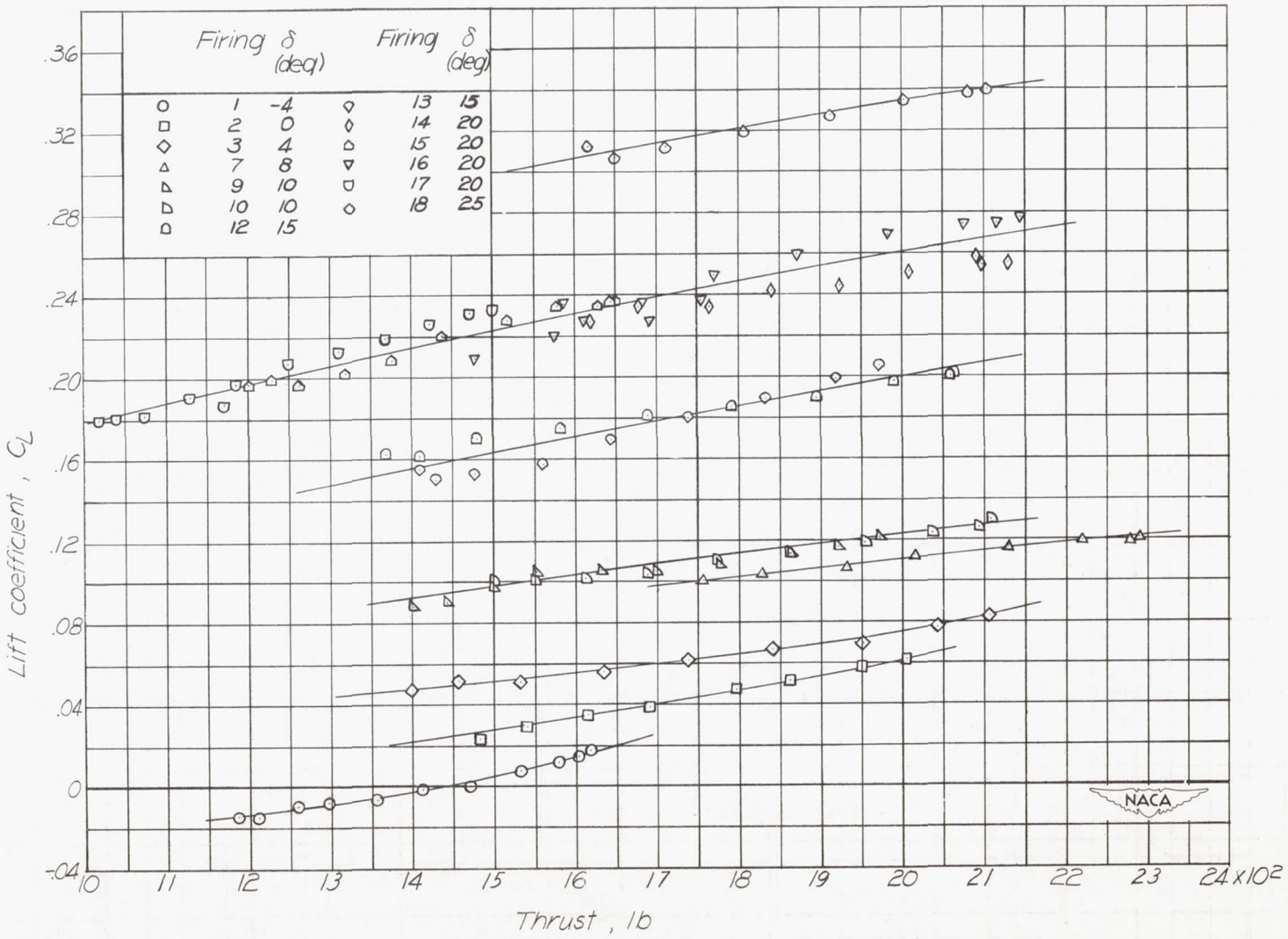


Figure 7.- Variation of lift coefficient with thrust for constant vane deflection angles. Vane aspect ratio, 2.

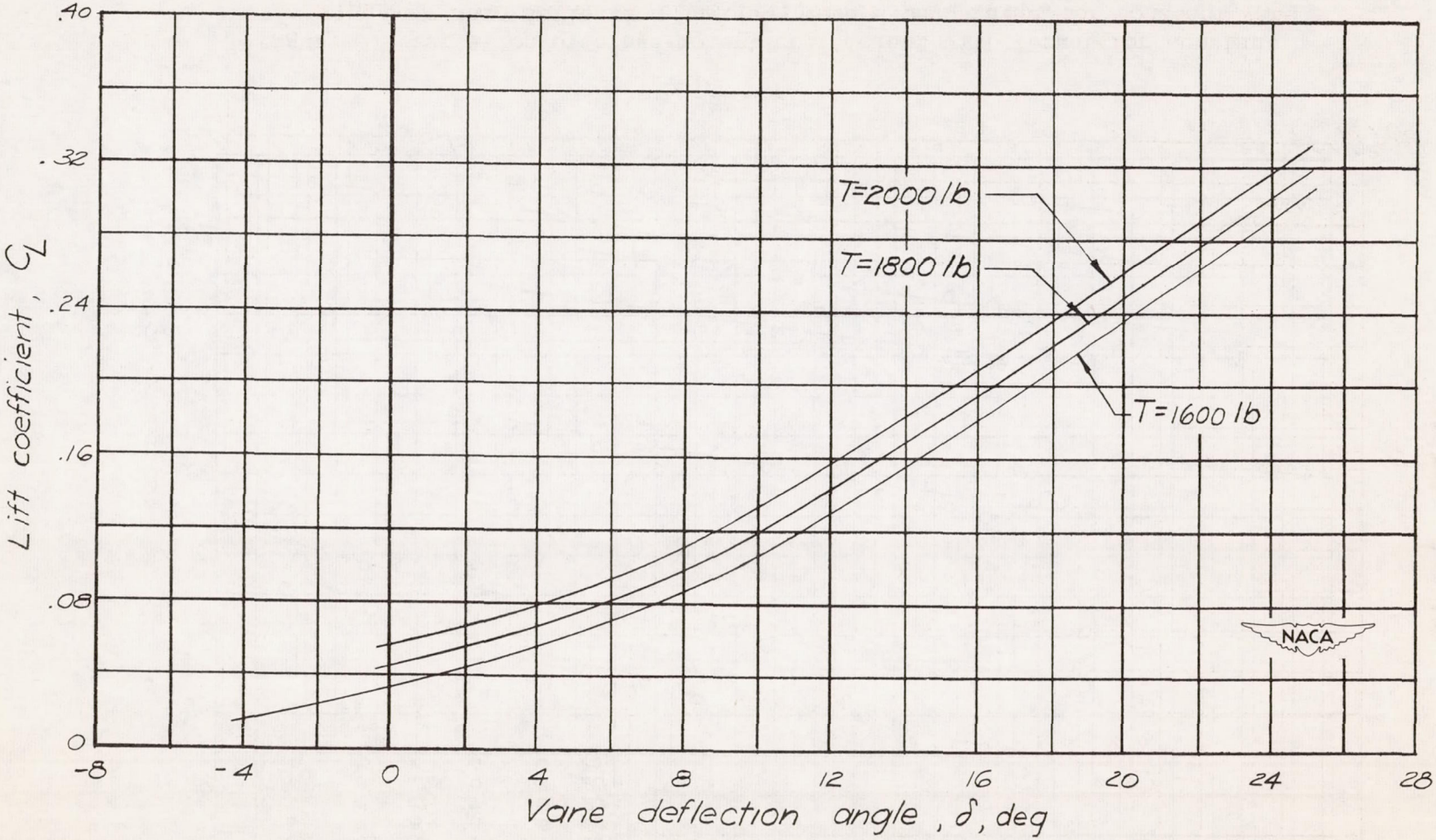


Figure 8.- Variation of lift coefficient with vane deflection angle for constant values of thrust. Vane aspect ratio, 2.

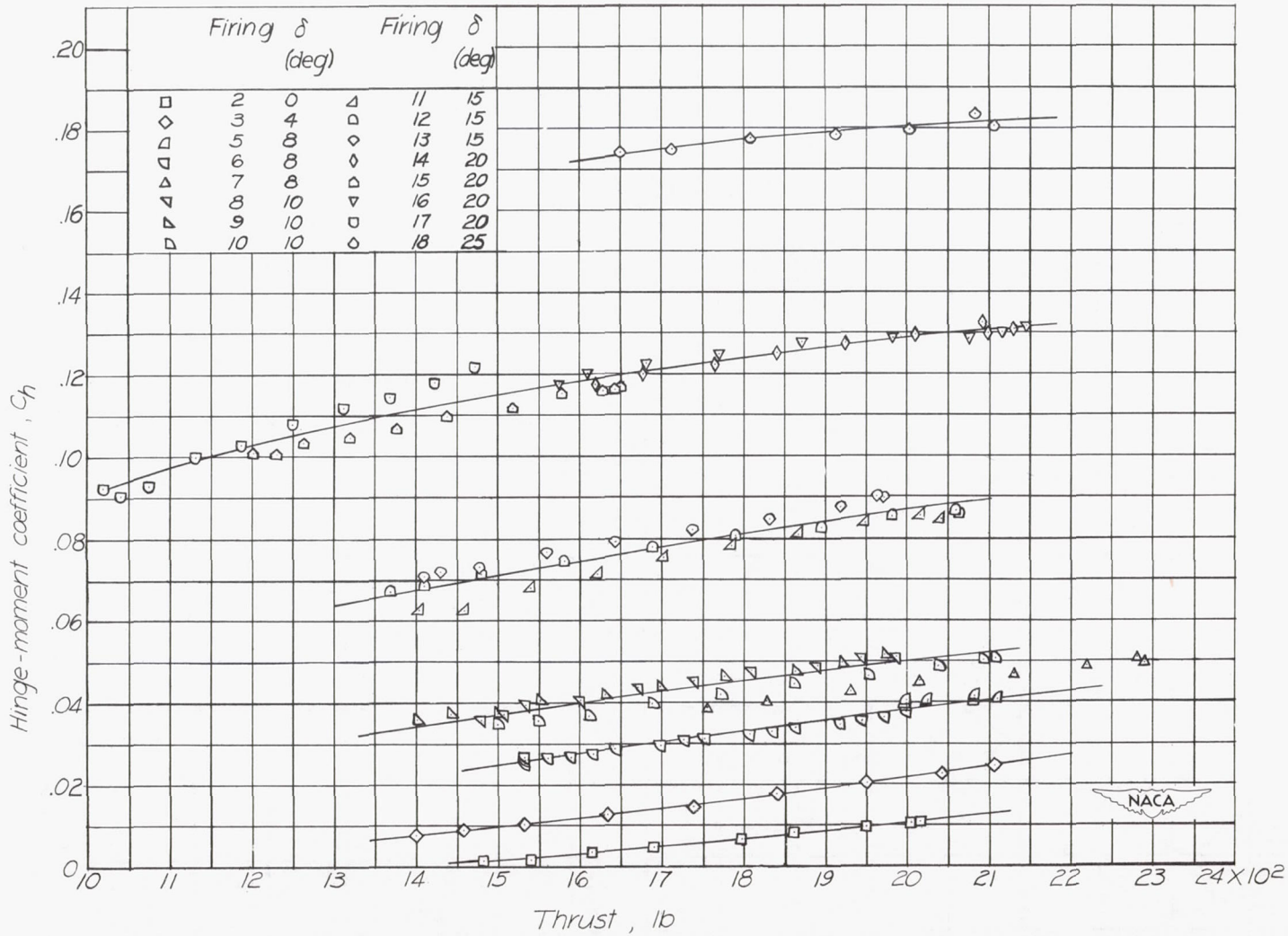


Figure 9.- Variation of hinge-moment coefficient with thrust for constant vane deflection angles. Vane aspect ratio, 2.

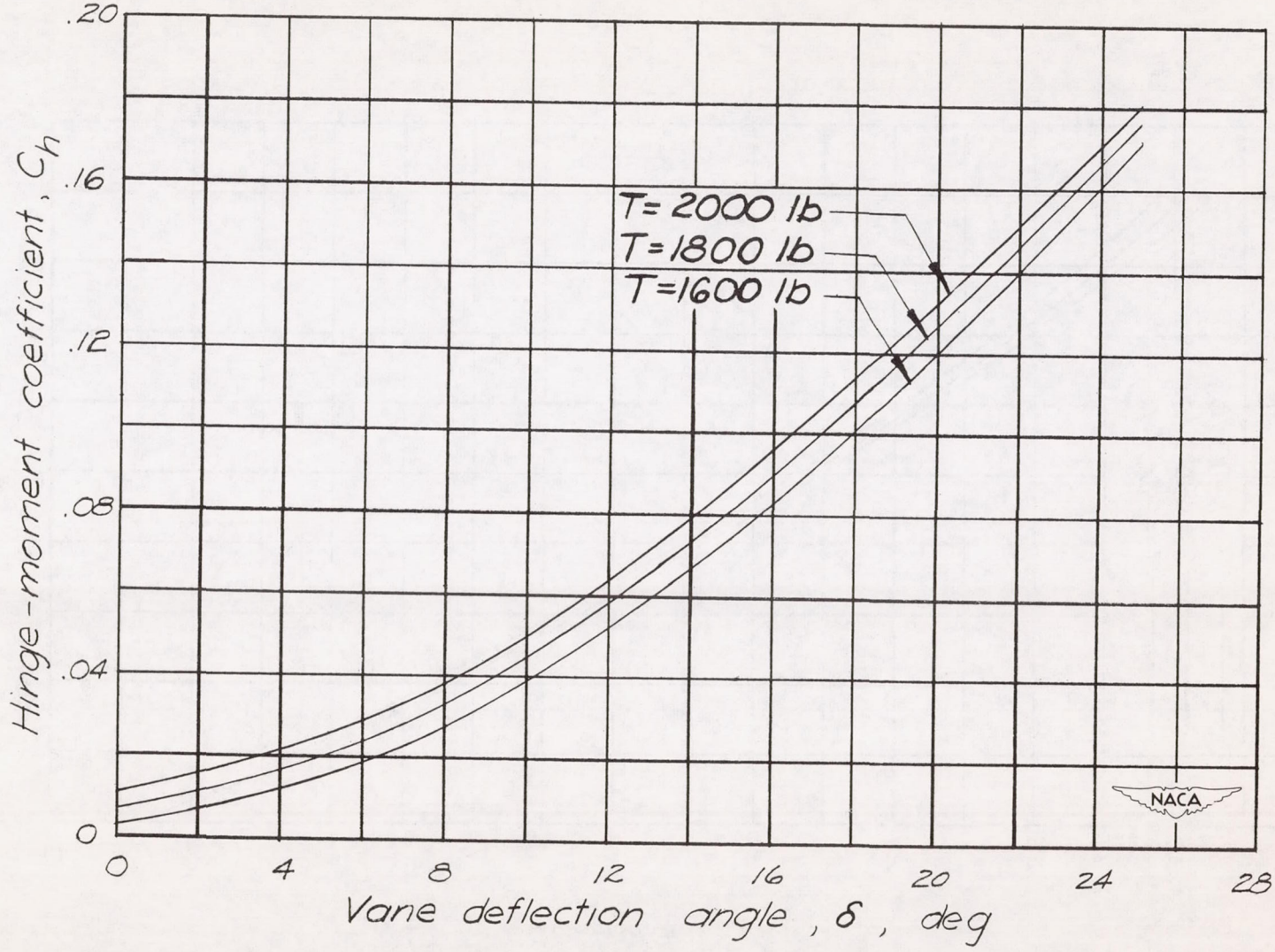


Figure 10.- Variation of hinge-moment coefficient with vane deflection angle for constant values of thrust. Vane aspect ratio, 2.



Figure 11.- Variation of lift coefficient with hinge-moment coefficient for constant values of thrust. Vane aspect ratio, 2.

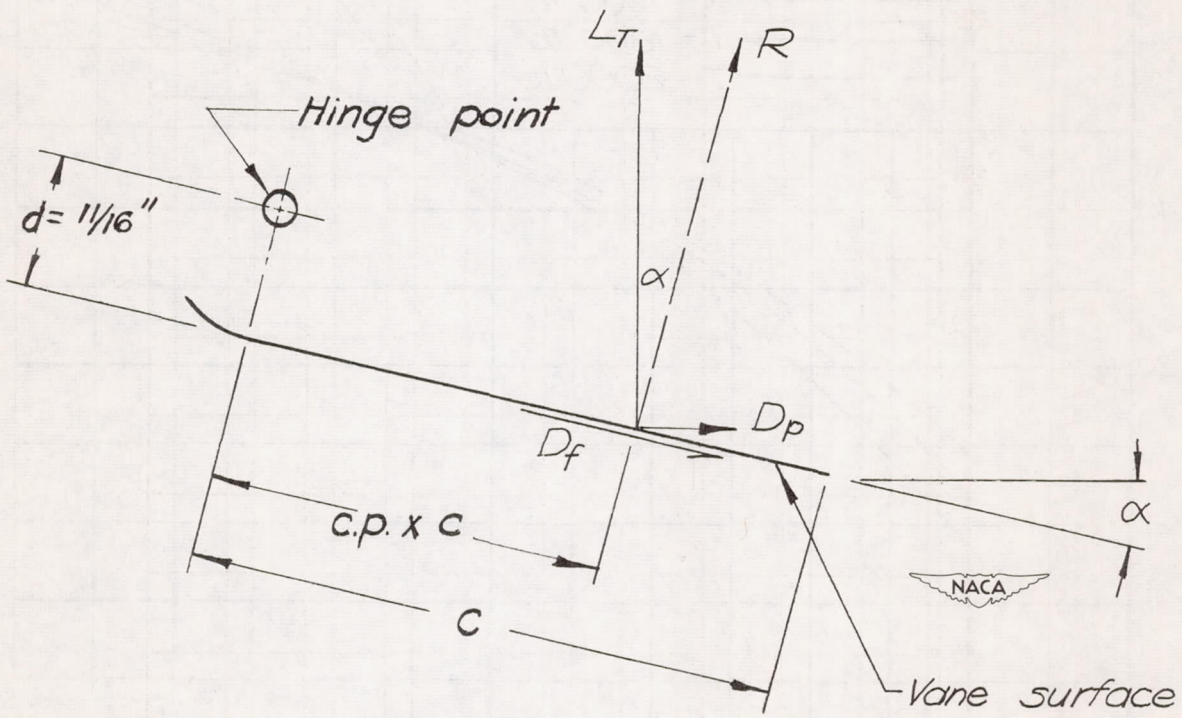


Figure 12.- Forces on jet vane.

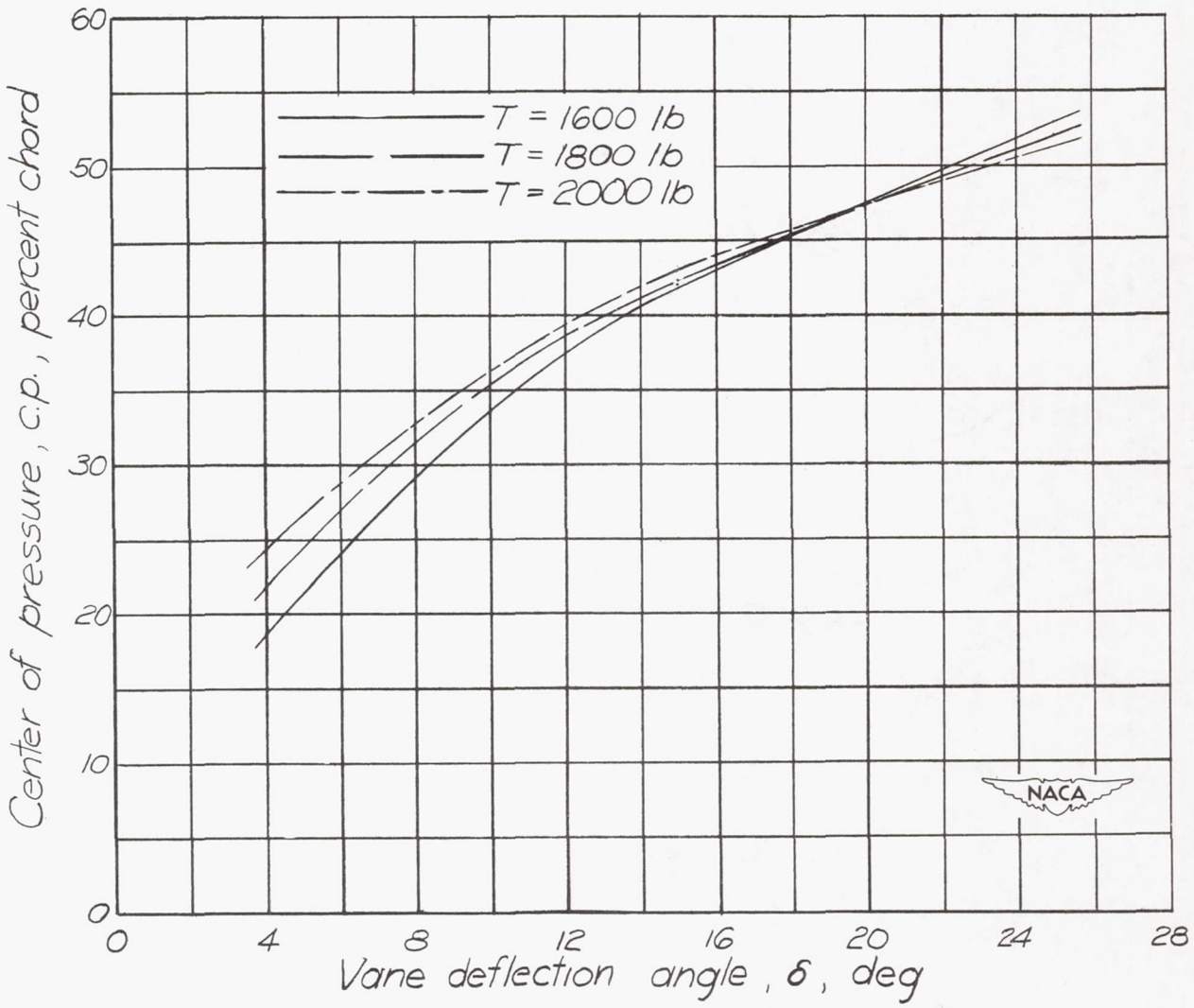
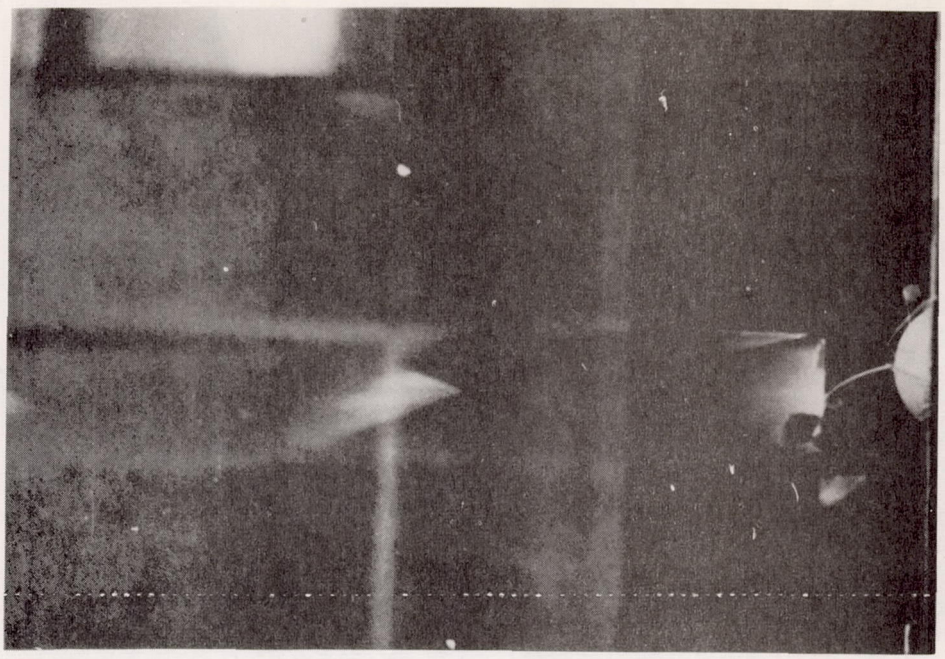
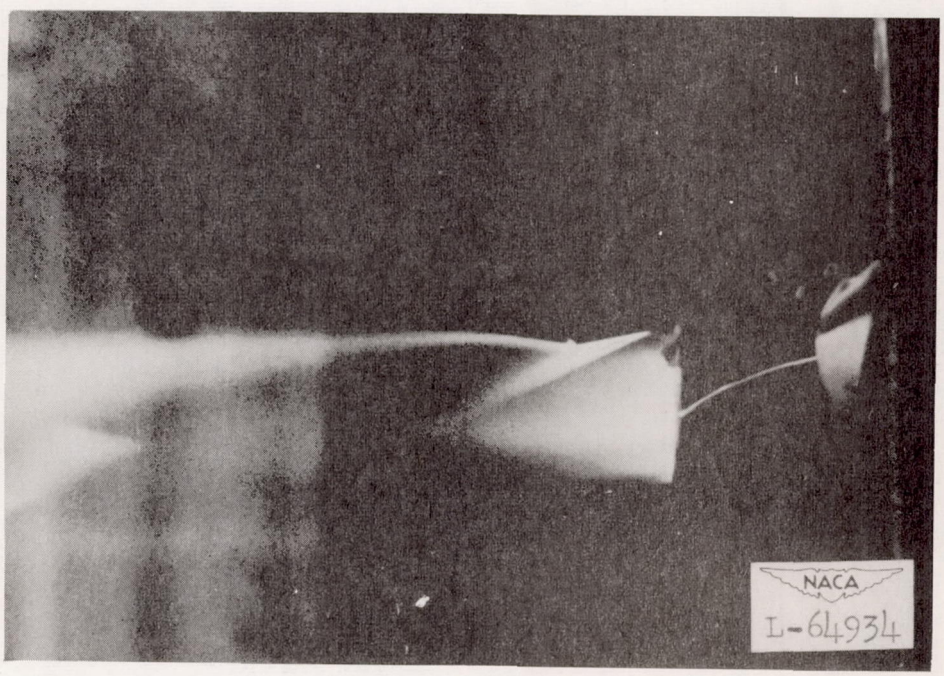


Figure 13.- Variation of center of pressure with vane deflection angle for constant thrust values. Vane aspect ratio, 2.



$\delta = 10^{\circ}$.



$\delta = 20^{\circ}$.

Figure 14.- Action of jet on vane for deflection angles of 10° and 20°. Vane aspect ratio, 2.

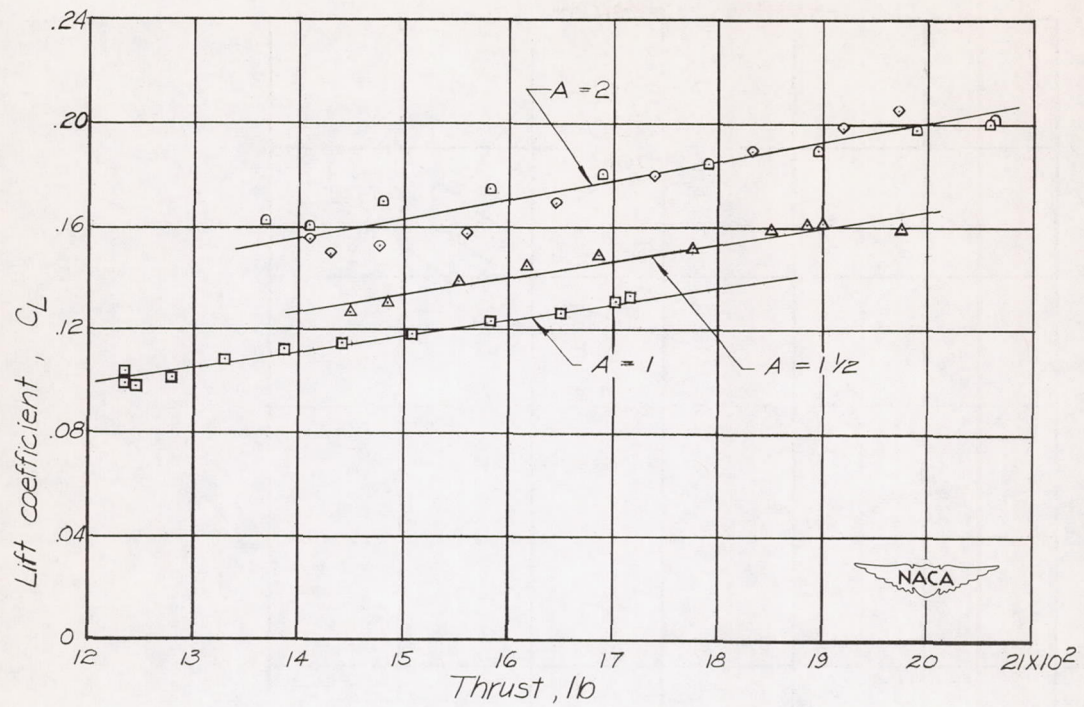


Figure 15.- Variation of lift coefficient with thrust for vanes of aspect ratio 1, $1\frac{1}{2}$, and 2. Vane span equals nozzle exit diameter; $\delta = 15^\circ$.

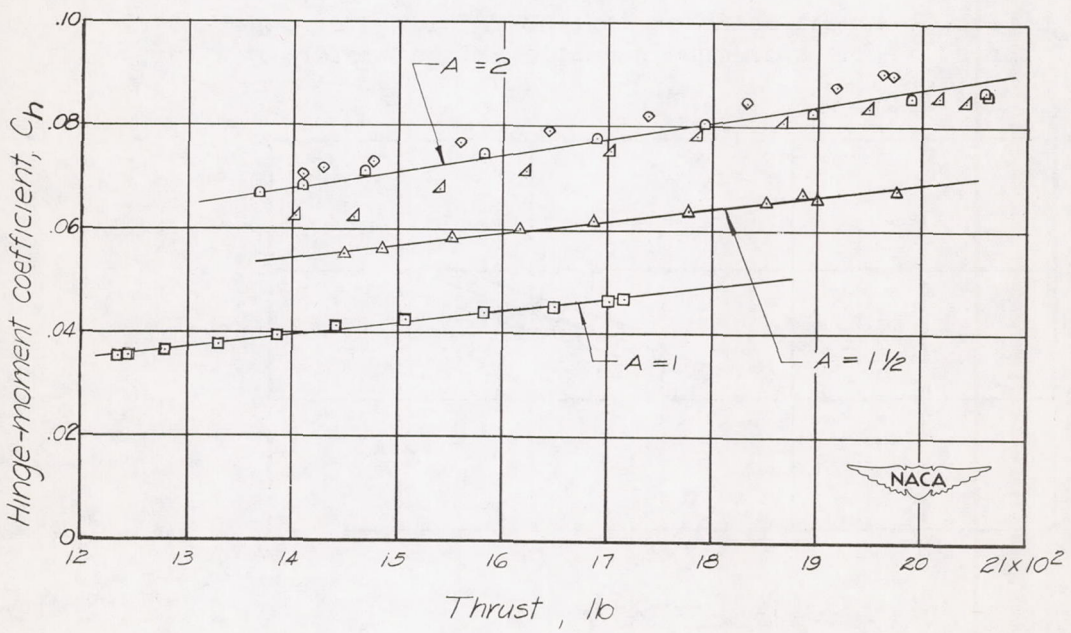


Figure 16.- Variation of hinge-moment coefficient with thrust for vanes of aspect ratio 1, $1\frac{1}{2}$, and 2. Vane span equals nozzle exit diameter; $\delta = 15^\circ$.

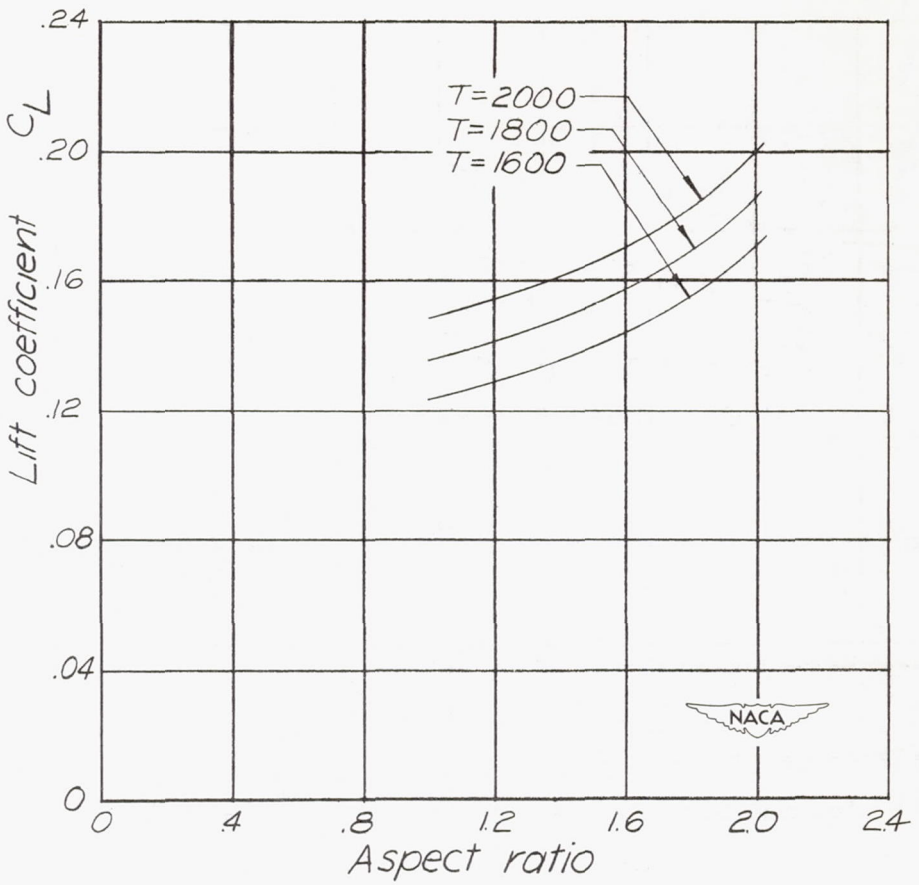


Figure 17.- Effect of aspect ratio on lift coefficient for constant values of thrust. Vane span equals nozzle exit diameter; $\delta = 15^{\circ}$.

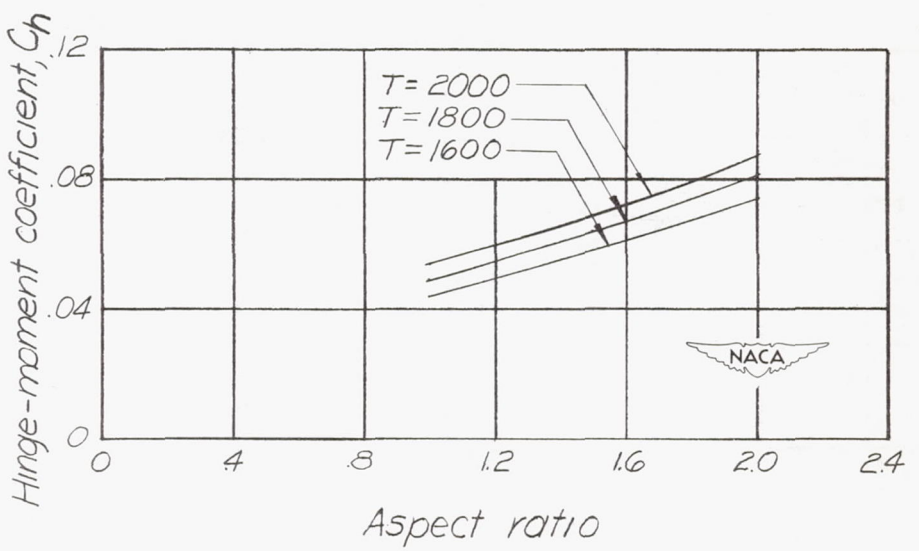


Figure 18.- Effect of aspect ratio on hinge-moment coefficient for constant values of thrust. Vane span equals nozzle exit diameter; $\delta = 15^{\circ}$.

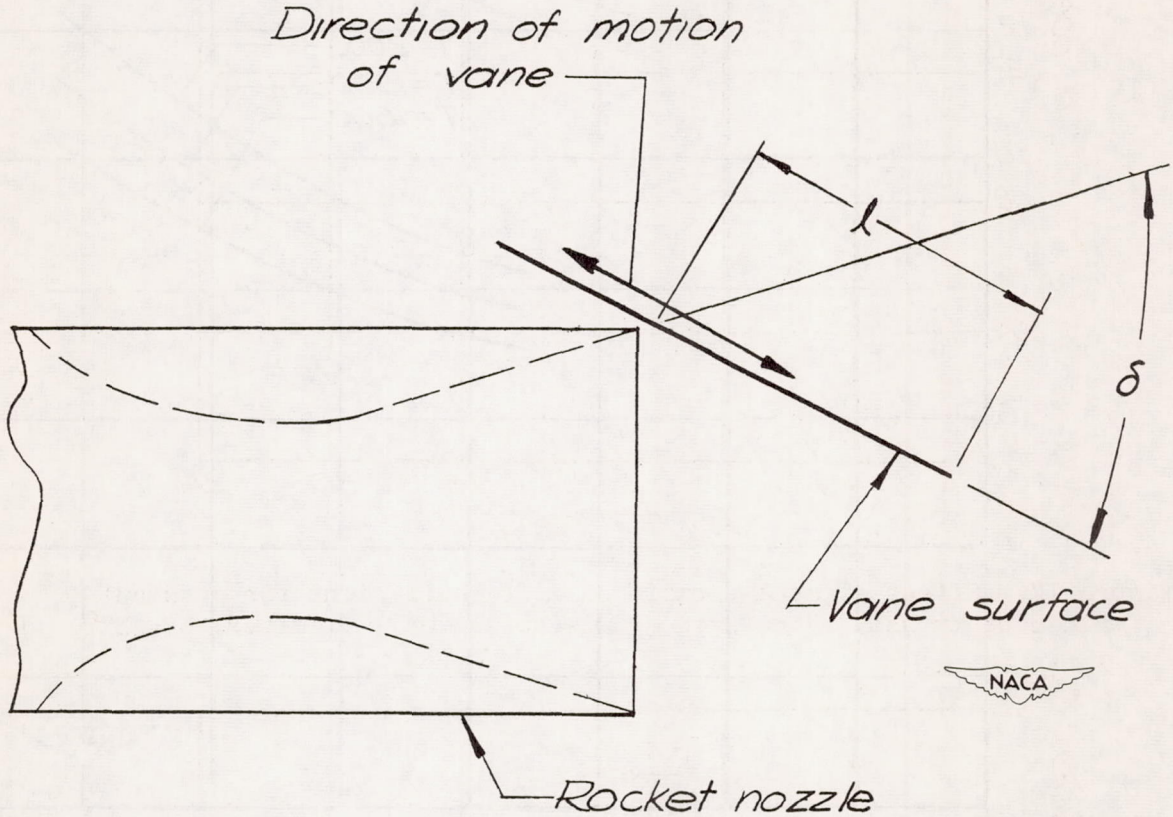


Figure 19.- Schematic sketch of variable immersion vane.

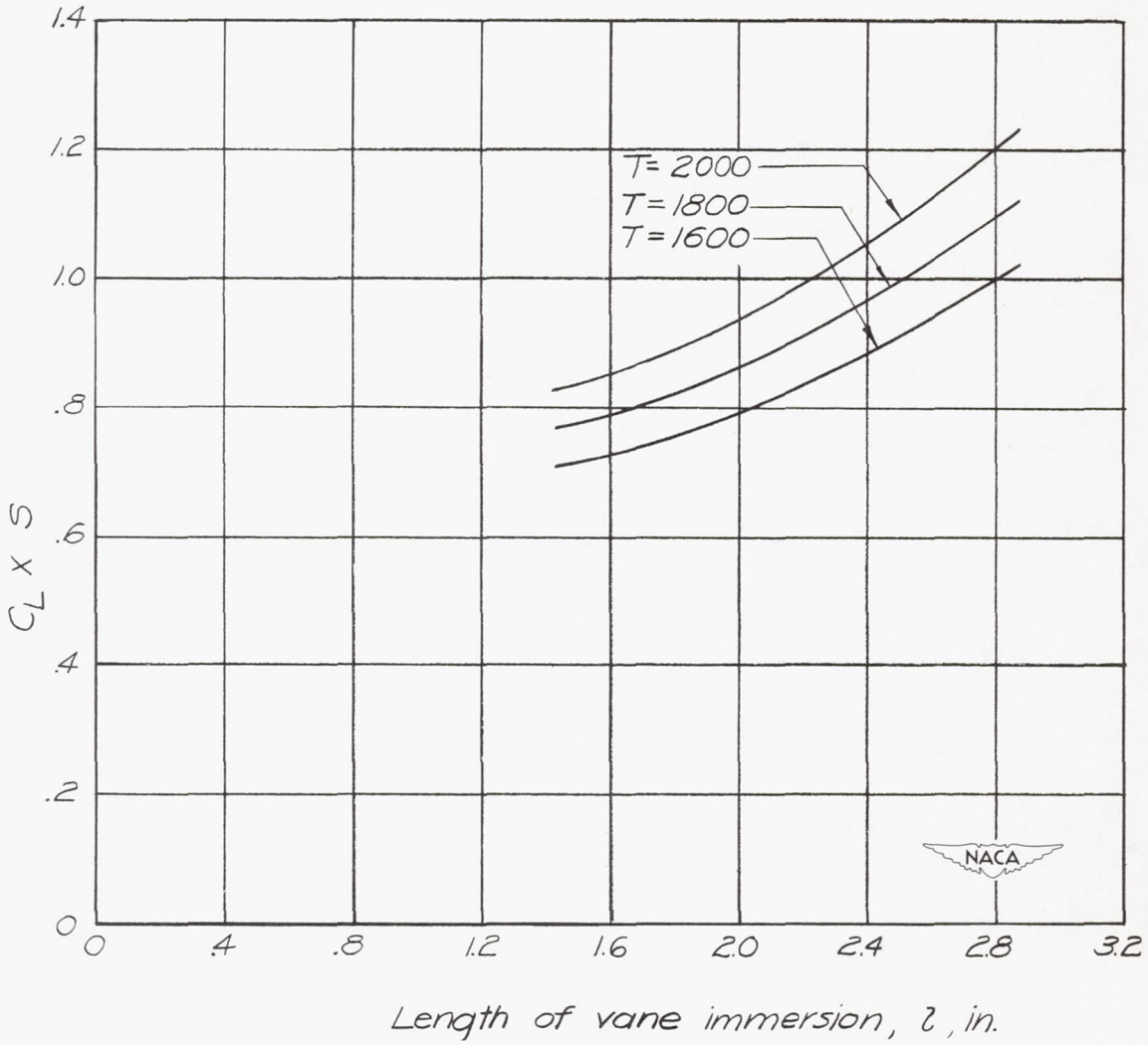


Figure 20.- Variation of lift coefficient times vane area with length of vane immersion for constant values of thrust. Vane span equals nozzle exit diameter; $\delta = 15^{\circ}$.

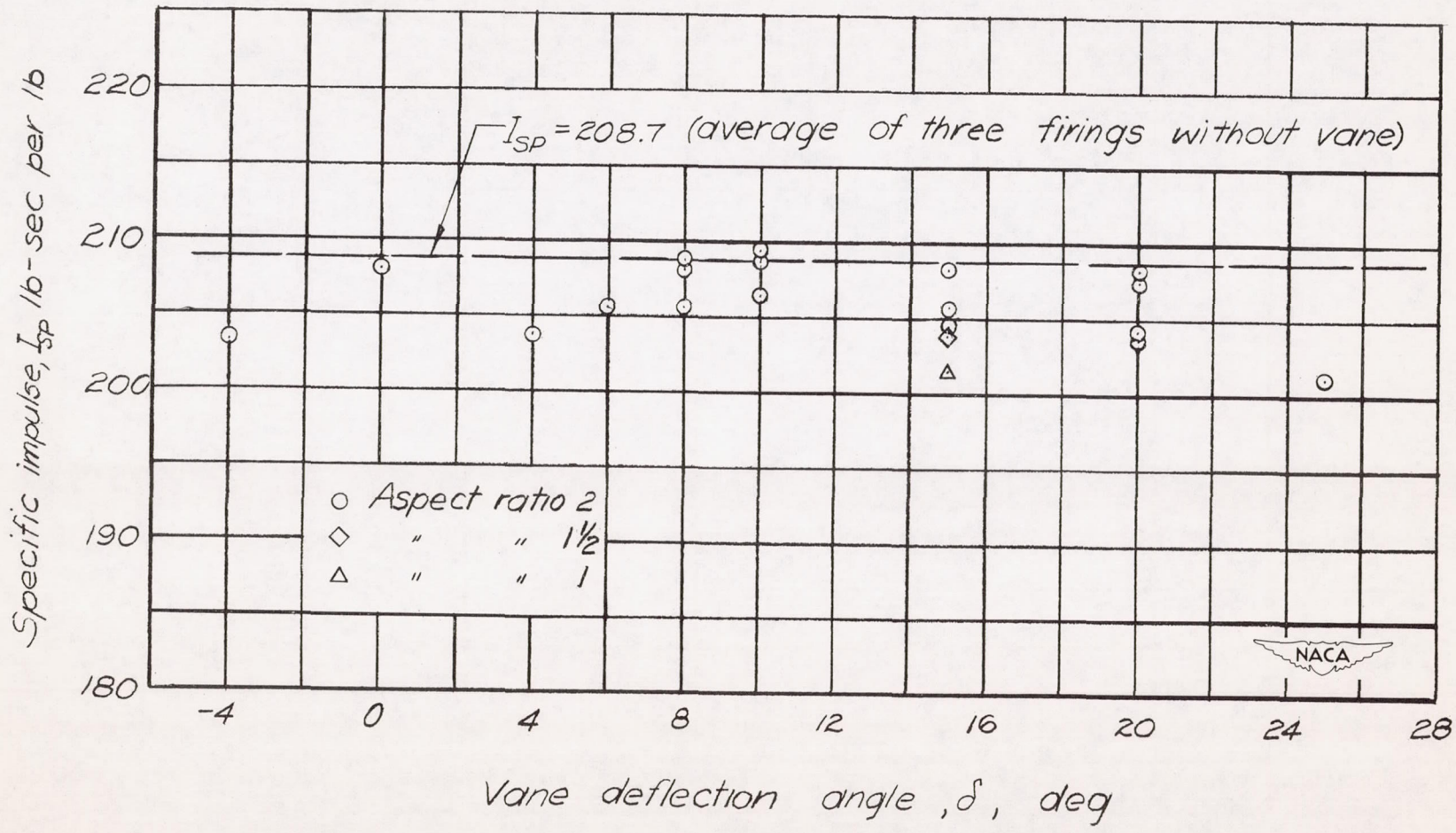


Figure 21.- Specific impulse realized from firings with jet vane at various deflection angles compared with an average of three firings without vane.